

Human derived dimerization tag enhances tumor killing potency of a T-cell engaging bispecific antibody

Mahiuddin Ahmed[†], Ming Cheng[†], Irene Y Cheung, and Nai-Kong V Cheung*

Department of Pediatrics; Memorial Sloan Kettering Cancer Center; New York, NY USA

[†]These authors equally contributed to this work.

Keywords: Bispecific antibody, BiTE, ganglioside, GD2, immunotherapy, melanoma, neuroblastoma, T-cell

Abbreviations: BiTE, bispecific T-cell engager; BsAb, bispecific antibody; HDD, HNF1 α dimerization domain; tsc-BsAb, tandem single-chain bispecific antibody.

Bispecific antibodies (BsAbs) have proven highly efficient T cell recruiters for cancer immunotherapy by virtue of one tumor antigen-reactive single chain variable fragment (scFv) and another that binds CD3. In order to enhance the antitumor potency of these tandem scFv BsAbs (tsc-BsAbs), we exploited the dimerization domain of the human transcription factor HNF1 α to enhance the avidity of a tsc-BsAb to the tumor antigen disialoganglioside GD2 while maintaining functional monovalency to CD3 to limit potential toxicity. The dimeric tsc-BsAb showed increased avidity to GD2, enhanced T cell mediated killing of neuroblastoma and melanoma cell lines *in vitro* (32–37 fold), exhibited a near 4-fold improvement in serum half-life, and enhanced tumor ablation in mouse xenograft models. We propose that the use of this HNF1 α -derived dimerization tag may be a novel and effective strategy to increase the potency of T-cell engaging antibodies for clinical cancer immunotherapy.

Bispecific antibodies (BsAbs) that engage T cells for antitumor immunotherapy have shown tremendous potential in animal studies and early clinical trials.¹ There exist a number of ways to construct BsAb formats that either utilizes the full immunoglobulin G (IgG) framework, single chain variable domains (scFv), or combinations thereof. One of the most clinically successful BsAb formats is a single polypeptide composed of 2 scFv units in tandem (tsc-BsAb), where one scFv binds to CD3 on the surface of T cells and the other scFv targets a tumor antigen. For CD19-positive leukemias and lymphomas, the tsc-BsAb of anti-CD19xanti-CD3 (termed Bispecific T cell Engager, BiTE) was highly effective in inducing T-cell mediated cytotoxicity and preventing tumor growth in xenograft studies.² In a human trial using the anti-CD19xanti-CD3 tsc-BsAb (Blinatumomab), major clinical benefits were seen, including partial and complete remissions.³ Blinatumomab was highly effective at extremely low doses (0.06 mg/m²/day) against pre-B-cell acute lymphoblastic leukemia (ALL) and non-Hodgkin's lymphoma with manageable cytokine storm toxicity.⁴ Bolus injections, however, can result in substantial central nervous system (CNS) toxicities, the underlying mechanisms of which are not well understood but may be

due to leakage of the antibody into the brain. In addition to the CD19xCD3 BiTE, other antibodies using the tsc-BsAb format have been developed to several human tumor targets, including MSCP (CSPG4) for melanoma,⁵ EpCAM for pancreatic CA,⁶ CEA for epithelial cancers,⁷ and EGFR for colorectal cancer.⁸ Despite these encouraging results, tsc-BsAbs have limitations. Their relatively small size (~55 kDa) predisposes tsc-BsAbs to succumb to rapid renal clearance, requiring continuous infusions over 4–8 weeks to achieve clinical effect. The modest size of these bivalent constructs may also facilitate their leakage into the CNS. An additional technical hurdle is that the monovalency of tsc-BsAbs toward the tumor antigen requires high affinity of the anti-tumor scFv to achieve optimal tumor epitope binding.

In this study we designed a novel platform to enhance the potency and efficacy of T-cell engaging tsc-BsAbs. We considered the ideal BsAb to have bivalent binding to the tumor antigen for enhanced avidity, and a molecular size of 100–120 kDa for optimal tumor penetration, tumor retention, and serum half-life.⁹ Given that excess cytokine release is a known side effect of BsAbs, we also considered the ideal BsAb to have functional monovalency of CD3 engagement in the absence of FcR(n) binding to

© Mahiuddin Ahmed, Ming Cheng, Irene Y Cheung, and Nai-Kong V Cheung

*Correspondence to: Nai-Kong V Cheung; Email: cheungn@mskcc.org

Submitted: 11/14/2014; Accepted: 11/15/2014

<http://dx.doi.org/10.4161/2162402X.2014.989776>

This is an Open Access article distributed under the terms of the Creative Commons Attribution-Non-Commercial License (<http://creativecommons.org/licenses/by-nc/3.0/>), which permits unrestricted non-commercial use, distribution, and reproduction in any medium, provided the original work is properly cited. The moral rights of the named author(s) have been asserted.

reduce recirculation and prolonged cytokine release. To accomplish these objectives, we engineered a human-derived homodimerization tag to increase the avidity of the bispecific antibody to the tumor target, optimizing serum half-life and potentially reducing leakage into the CNS, while increasing T cell mediated antitumor potency without excessive cytokine release. We chose to use the dimerization domain of human hepatocyte nuclear factor 1 α , HNF1 α (residues 1–32), which forms a tightly wound anti-parallel 4 helix bundle in the dimer conformation.¹⁰ Using this human dimerization sequence, we engineered bivalent binding of the tsc-BsAbs to their tumor targets without introducing immunogenicity. Given that the anti-parallel orientation of the HNF1 α dimerization domain would orient any attached domain in the opposite direction, CD3 engagement was designed to be functionally monovalent, a property crucial for the clinical safety of this dimeric BsAb platform.

To test the utility of this HNF1 α dimerization domain (HDD), we constructed tsc-BsAb against the carbohydrate epitope on disialoganglioside antigen GD2, a proven tumor target on the cell surface of a broad spectrum of human cancers.^{11–13} These tumors include neuroblastoma, soft tissue sarcomas, osteosarcoma, small cell lung cancer, melanoma, retinoblastoma, and brain tumors. More recently, several laboratories have reported the presence of GD2 on breast cancer stem cells,^{14,15} neuroectodermal¹⁶ and mesenchymal stem cells.^{17,18} The anti-GD2 \times anti-CD3 tsc-BsAb (GD2 \times CD3) were composed of single

polypeptide chains containing the scFv of anti-GD2 monoclonal antibody 5F11^{19–21} and the humanized scFv of the anti-CD3 antibody OKT3²² without and with the HNF1 α dimerization domain (HDD) (see Fig. 1A and 1B). We previously described the potency of this 5F11 GD2 \times CD3 monomeric BsAb against GD2-positive tumor cell lines and tumor xenografts.²¹ The HDD tag was placed at the carboxyl end of anti-CD3 scFv and distal to the anti-GD2 scFv. This was done to maximize the functional affinity for the tumor antigen (GD2) at the N-terminal end of the molecule, but not to CD3, since the anti-CD3 scFvs were sterically restricted due to the anti-parallel arrangement of the HDD helices, which would orient the anti-CD3 scFvs $\sim 180^\circ$ apart.¹⁰ Enhancement of GD2 binding would potentially enhance tumor killing, whereas enhancement of CD3 binding could lead to anergy or overactivation of T cells causing cytokine storm. The molecular size of the dimerized tsc-BsAb (MW ~ 118 kDa) would increase to above the renal clearance threshold (~ 60 kDa), thereby enhancing serum half-life. We compared the HDD tag with 2 other homo-dimerization domains: the synthetic helix-loop-helix (dHLX) peptide²³ which has previously been shown to form an anti-parallel 4 helical bundle that can dimerize scFv fragments, and the human IgG1-Fc domain which forms covalent homodimers (see Fig. 1C and 1D).

We focused our investigation on enhancing the properties of the tsc-BsAb format because it has demonstrated the highest T cell engaging potency compared to other published formats (see

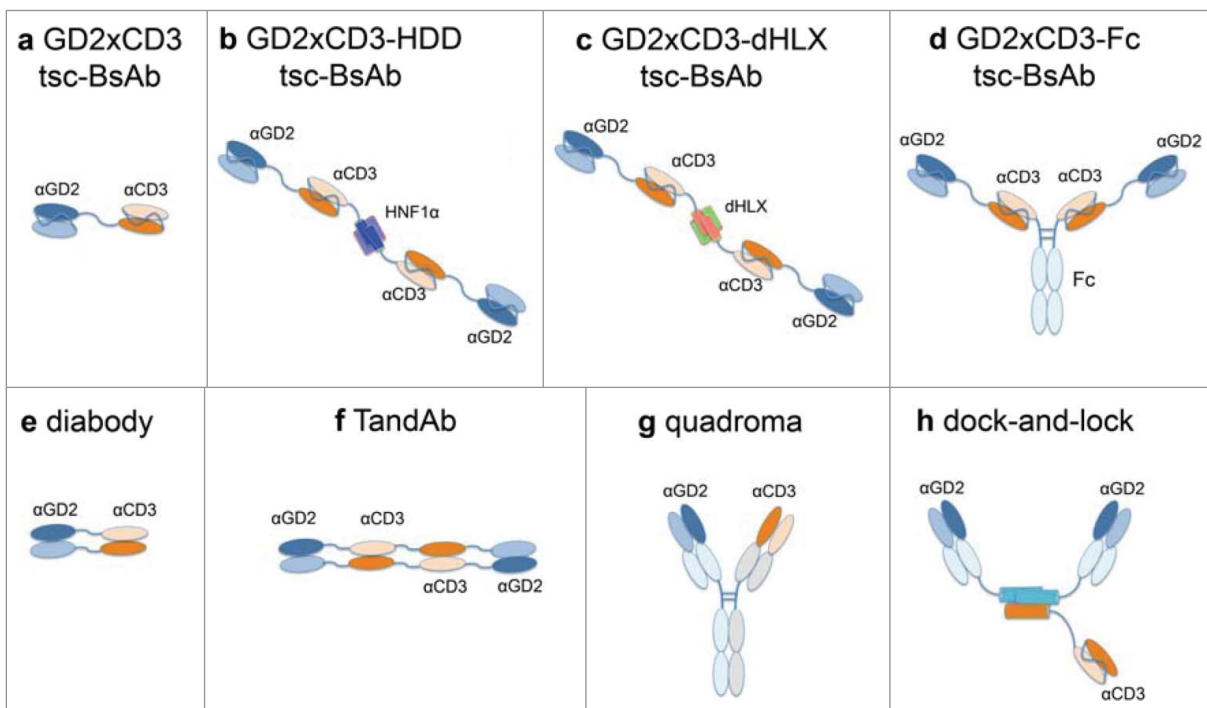


Figure 1. Engineering bispecific antibodies for cancer immunotherapy. Bispecific antibody formats that were compared in this investigation include: (A) GD2 \times CD3 tandem single chain variable fragment (scFv) bispecific antibody (BsAb) (tsc-BsAb) monomer, (B) GD2 \times CD3-HDD dimer generated by the addition of the hepatocyte nuclear factor 1 α (HNF1 α) dimerization domain (HDD) to C-terminus which forms an anti-parallel 4 helix bundle, (C) GD2 \times CD3-dHLX dimer using a synthetic helix-loop-helix domain (dHLX²³), (D) GD2 \times CD3-Fc dimer using a human IgG1 hinge and CH2 and CH3 domains. Other possible bispecific antibody formats considered: (E) diabody²⁴ (non-covalently associated dimers in which each chain comprises 2 domains consisting of VH and VL domains from 2 different antibodies), (F) tandem diabody²⁵ (TandAb), (G) quadromas (IgG like BsAbs formed by hybrid hybridomas²⁶ or by engineering Fc heterodimers²⁷), and (H) Dock-and-Lock²⁸ BsAbs (covalent trimer of 2 antitumor Fab fragments and one anti-CD3 scFv).

Table 1. Bispecific antibody (BsAb) biophysical characterization by Dynamic Light Scattering (DLS), Size Exclusion Chromatography (SEC), and Surface Plasmon Resonance (SPR).

BsAb Construct	Yield (mg/L culture)	Diameter (nm \pm SD)DLS	Purity (by HPLC-SEC)	K_{on} (1/Ms)SPR	K_{off} (1/s)SPR	K_D SPR
GD2xCD3	2	7.2 \pm 1.7	95%	9.07 \times 10 ⁴	2.27 \times 10 ⁻²	250 nM
GD2xCD3-HDD	4	11.1 \pm 0.5	97%	8.83 \times 10 ⁴	3.45 \times 10 ⁻³	39 nM

Fig. 1E-H) such as the diabody²⁴ (non-covalently associated dimers in which each chain comprises 2 domains consisting of VH and VL domains from 2 different antibodies), tandem diabody²⁵ (TandAb), quadromas (IgG-like BsAbs formed by hybrid hybridomas²⁶ or by engineering Fc heterodimers²⁷), and Dock-and-Lock²⁸ BsAbs (covalent trimer of 2 antitumor Fab fragments and one anti-CD3 scFv). Direct comparison showed that the tsc-BsAb BiTE format (CD19xCD3) was 700–8000 fold more potent than the tandem diabody,²⁹ which in turn was superior to diabodies or quadromas²⁵ at redirecting T cells to kill B cell lymphoma cell lines. The superiority of BiTE format over diabody was independently confirmed using the EGFRxCD3 BsAb,³⁰ strongly suggestive of a structural preference of the tsc-BsAb format for efficient T-cell engagement. More recently, the CD19xCD19xCD3 Dock-and-Lock BsAb²⁸ was generated, but it too showed significantly weaker tumor cytotoxicity when compared to the published cytotoxicity of the BiTE format described by Molhoj et al.²⁹ We therefore chose the tsc-BsAb format to test the dimerization tag HDD. Here, we present biophysical data on the dimerization and *in vitro* binding kinetics of the HDD-tagged GD2xCD3 BsAb, and *in vitro* T cell-mediated tumor cell killing, as well as *in vivo* antitumor effects using mouse xenograft models.

Results

HDD-tag induced BsAb dimerization and enhanced avidity to tumor antigen GD2

The ability of the HDD tag to induce dimerization was assayed by dynamic light scattering and size exclusion chromatography (see Table 1 and Fig. S1). GD2xCD3 BsAb (MW 54 kDa) had a diameter of 7.2 \pm 1.7 nm and was 95% monomeric, whereas GD2xCD3-HDD BsAb (MW 59 kDa for monomer, 118 kDa for dimer) had a diameter of 11.1 \pm 0.5 nm and was 97% dimeric. In addition to higher purity, the GD2xCD3-HDD BsAb had a 2-fold increase in yield when stably expressed in CHO cells.

To test whether the HDD tag enhanced the functional affinity to tumor antigen GD2, Surface Plasmon Resonance (SPR) and ELISA experiments were done using purified GD2 (Table 1, Fig. 2 and Table 2). SPR analysis showed that the K_{on} for GD2xCD3 BsAb and GD2xCD3-HDD BsAb were similar (9.07 \times 10⁴ 1/Ms and 8.83 \times 10⁴ 1/Ms, respectively), but the K_{off} were very different (2.27 \times 10⁻² 1/s and 3.45 \times 10⁻³ 1/s, respectively). This resulted in a 6-7 fold difference in the overall K_D (250 nM for GD2xCD3 BsAb and 39 nM for GD2xCD3-HDD BsAb). The kinetic analysis confirmed that the HDD tag enhanced the ability of the BsAb to retain its distal target. ELISA binding assays showed an 8-fold enhancement of GD2 binding

for GD2xCD3-HDD BsAb when compared with GD2xCD3 BsAb. We also compared the HDD tag to the synthetic dHLX and the human Fc domain. To this end, GD2xCD3 BsAb was produced with either the HDD, dHLX domain, or the Fc domain at their respective C-termini and assayed for GD2 antigen binding (Table 2 and Fig. 2C). The GD2 binding showed that covalent dimers formed by GD2xCD3-Fc BsAb (0.3 nM EC₅₀, 99% dimeric by HPLC-SEC) had a two-fold enhancement in avidity to GD2, when compared with the non-covalent dimers formed by GD2xCD3-HDD BsAb (0.6 nM EC₅₀). ELISA results showed that binding of both of these constructs were several fold higher than monomeric GD2xCD3 BsAb (5.0 nM

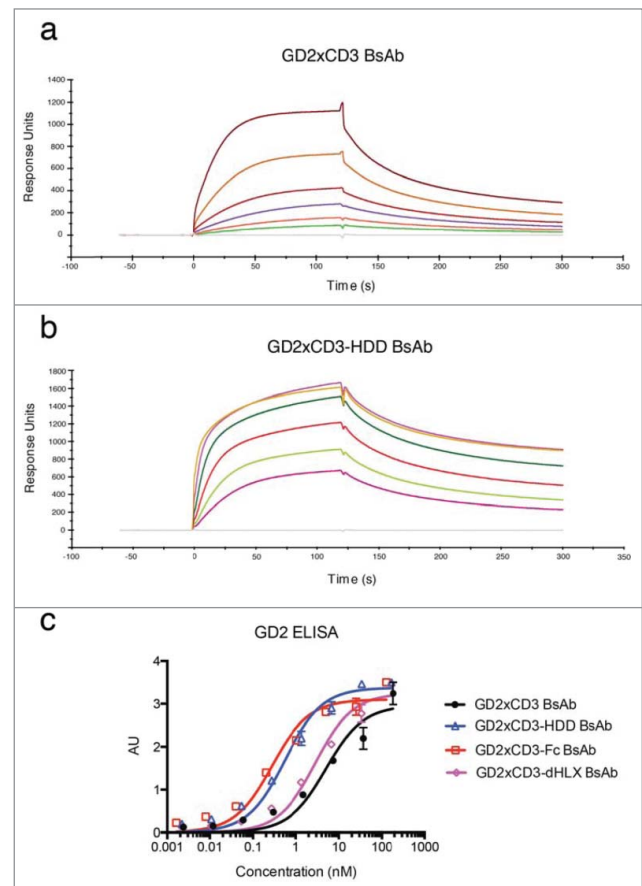


Figure 2. Comparison of bispecific antibody GD2 tumor antigen-binding kinetics. Bispecific antibody GD2 binding kinetics by surface plasmon resonance of (A) GD2xCD3 BsAb and (B) GD2xCD3-HDD. Traces are shown at the following BsAb concentrations: 62.5, 125, 250, 500, 1000, and 2000 nM. Analyses of the association and dissociation rates are shown in Table 1. (C) Binding to tumor antigen GD2 by ELISA for 4 BsAb constructs. Data are shown as the mean \pm SD. The resultant EC₅₀ of binding are shown in Table 2.

Table 2. Analysis of binding of the indicated bispecific antibody (BsAb) to GD2 tumor antigen by ELISA (mean \pm SE).

BsAb Construct	GD2 binding EC50 (nM)	Relative binding	P-value
GD2xCD3	5.0 \pm 1.4	1	-
GD2xCD3-HDD	0.6 \pm 0.1	8.3	<0.0001
GD2xCD3-Fc	0.3 \pm 0.1	16.7	<0.0001
GD2xCD3-dHLX	2.9 \pm 0.6	1.7	0.1982

Table 3. Analysis of binding of the indicated bispecific antibody (BsAb) to CD3 on T cells by cytofluorimetric analysis (mean \pm SE).

BsAb Construct	CD3 binding EC50 (nM)	Maximal binding (AU)	P-value
GD2xCD3	42 \pm 21	14.0 \pm 2.4	-
GD2xCD3-HDD	73 \pm 23	16.7 \pm 2.2	0.6963
GD2xCD3-Fc	24 \pm 3.6	18.2 \pm 0.8	0.0043
GD2xCD3-dHLX	poor fit	poor fit	NA

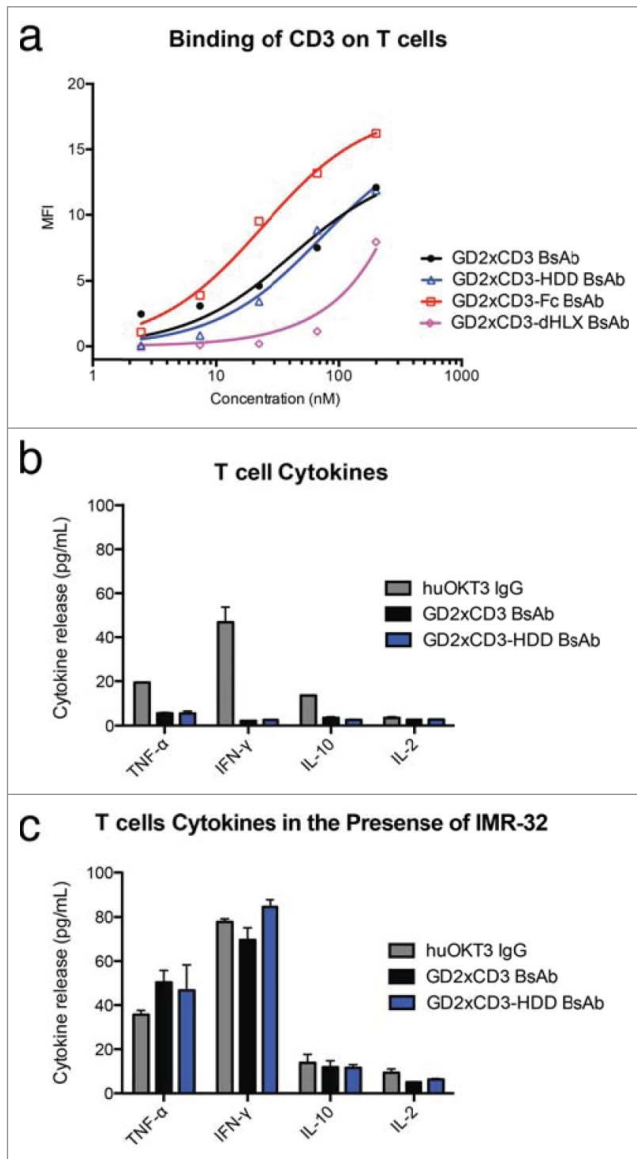


Figure 3. Bispecific antibody binding to human T cell CD3 and cytokine release. T cells purified from human peripheral blood mononuclear cells were incubated with the indicated bispecific antibody (BsAb) and characterized for CD3 binding (cytofluorimetric analysis) and cytokine release (ELISA). (A) Binding of GD2xCD3, GD2xCD3-HDD, GD2xCD3-Fc, and GD2xCD3-dHLX BsAbs to CD3 on the surface of T cells by flow cytometry. (B) Cytokine release from T cells induced by GD2xCD3 and GD2xCD3 BsAb when compared with a huOKT3 IgG. (C) Cytokine release from T cells co-cultured with neuroblastoma IMR-32 cells in the presence of the indicated BsAb. Data points are shown as mean \pm SD. Cytokine values and statistical analyses are shown in **Table S1** and **Table S2**.

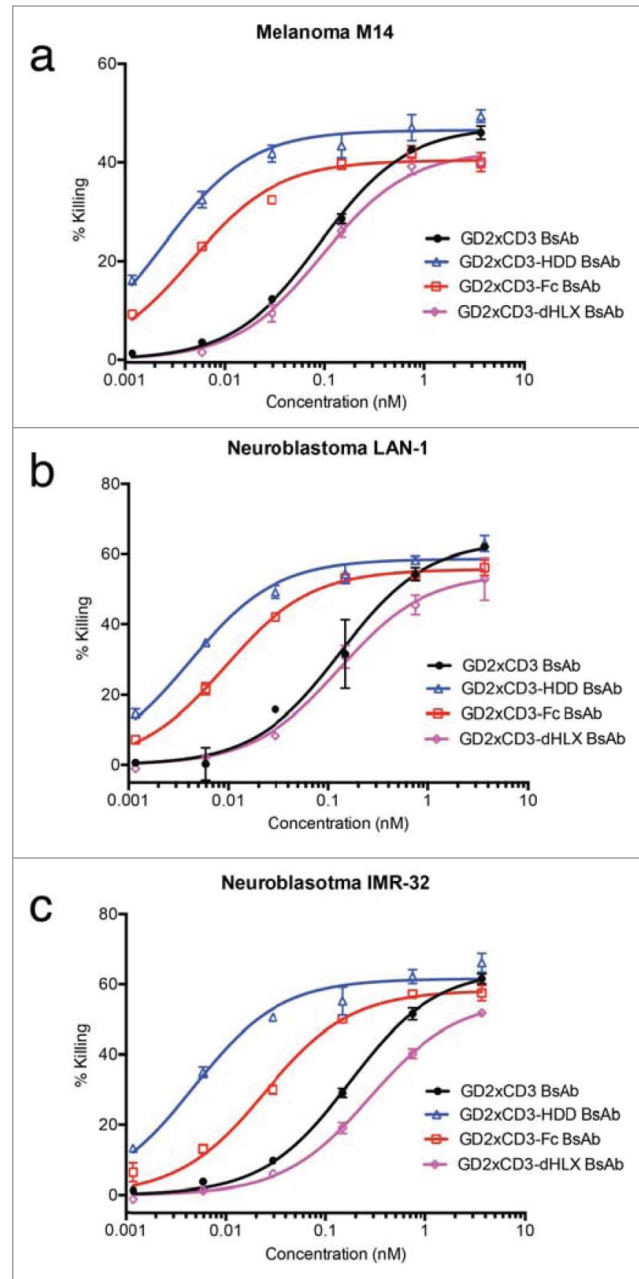


Figure 4. Bispecific antibody stimulated T cell-mediated cancer cell cytotoxicity. T cells purified from human peripheral blood mononuclear cells were incubated with the indicated bispecific antibody (BsAb) in the presence of cancer cells. T cell-mediated killing of (A) M14 melanoma, (B) LAN-1 neuroblastoma, and (C) IMR-32 neuroblastoma cells lines was analyzed by chromium⁵¹-release assay. Data are shown as the mean \pm SD. The EC50, maximal killing, and statistical analyses are shown in **Table 4**.

Table 4. Analysis of the indicated bispecific antibody (BsAb) to stimulate T cell-mediated cytotoxicity *in vitro* (mean \pm SE).

	GD2xCD3	GD2xCD3-HDD	GD2xCD3-Fc	GD2xCD3-dHLX
M14 Max Killing	46%	49%	40%	40%
M14 EC50 (pM)	89 \pm 4.1	2.4 \pm 0.3	4.7 \pm 0.4	94 \pm 8.5
Relative Potency	1	37	19	0.9
P-value EC50		<0.0001	<0.0001	0.5771
LAN-1 Max Killing	62%	63%	56%	53%
LAN-1 EC50 (pM)	131 \pm 22	4.1 \pm 0.4	9.2 \pm 0.5	129 \pm 17
Relative Potency	1	32	14	1
P-value EC50		<0.0001	<0.0001	0.9240
IMR-32 Max Killing	62%	66%	58%	52%
IMR-32 EC50 (pM)	175 \pm 9	4.8 \pm 0.6	24.4 \pm 2.2	278 \pm 15
Relative Potency	1	36	7	0.6
P-value EC50		<0.0001	<0.0001	<0.0001

EC₅₀) or the GD2xCD3-dHLX (2.9 nM EC₅₀). GD2xCD3-dHLX BsAb did not form homogeneous dimers, and contained >50% aggregates by HPLC-SEC analysis.

CD3 binding, cytokine release, and T-cell proliferation

We also compared T cell CD3 binding by fluorescence cytometry for all 4 constructs (GD2xCD3, GD2xCD3-HDD, GD2xCD3-dHLX, GD2xCD3-Fc BsAbs) (Fig. 3A and Table 3) and found no significant difference between the binding GD2xCD3 and GD2xCD3-HDD BsAbs ($P = 0.6963$), indicating functional monovalency to CD3. GD2xCD3-Fc BsAb showed significantly higher CD3 binding ($P = 0.0043$), with a nearly 2-fold decrease in EC50. This result indicates that the orientation of the anti-CD3 scFv fragments (HDD tagged versus Fc-tagged) can directly influence CD3 binding avidity. The GD2xCD3-dHLX BsAb showed the lowest CD3 binding, likely due to the observation that the sample did not form homogeneous dimers and contained aggregates.

We also characterized the ability of GD2xCD3 and GD2xCD3-HDD BsAb to induce T-cell mediated cytokine release in the presence or absence of GD2-expressing tumor cells (Fig. 3C and 3D, Table S1 and Table S2). The BsAb stimulated release of the cytokines tumor necrosis α (TNF α), interferon γ (IFN γ) and the interleukins IL10 and IL2 were measured. GD2xCD3-HDD BsAbs stimulated comparable cytokine release as GD2xCD3 (i.e., there was no significant difference), suggesting that although GD2xCD3-HDD dimer has 2 anti-CD3 moieties, it functions as a monovalent binder in regards to CD3-mediated cytokine release. When huOKT3 IgG (which is known to have 2 anti-CD3 moieties) was included in the cytokine release assay, it induced substantially more cytokine release than either of the GD2xCD3 or GD2xCD3-HDD BsAbs in the absence of tumor cells (Fig. 3B). However, in the presence of tumor cells a robust cytokine release was observed in the presence of all the BsAbs tested, with no appreciable difference observed between that induced by the monomer vs. the HDD-dimeric form (Fig. 3C).

We also compared the ability of GD2xCD3 and GD2xCD3-HDD BsAbs to induce CD3-mediated T cell proliferation as compared to huOKT3 IgG (Fig. S2). T-cell proliferation was

robust in the presence of huOKT3 IgG, while it was negligible when GD2xCD3 or GD2xCD3-HDD BsAbs were used.

T cell-mediated killing of tumor cells *in vitro*

All four BsAb constructs (GD2xCD3, GD2xCD3-HDD, GD2xCD3-Fc, GD2xCD3-dHLX) were tested for their ability to mediate T-cell killing of GD2-positive tumor cell lines, namely melanoma M14, and the neuroblastomas LAN1 and IMR-32 (Fig. 4 and Table 4). As compared to the GD2xCD3 BsAb, GD2xCD3-HDD showed the most significant enhancement in T-cell mediated killing of tumor cells in all 3 cell lines tested (32–37 fold increase, $P < 0.0001$), whereas GD2xCD3-Fc BsAb augmented target cell death more modestly, albeit significantly (7–19 fold, $P < 0.0001$). Interestingly, the killing by GD2xCD3-Fc BsAb was lower, despite having higher GD2 binding than GD2xCD3-HDD (Table 2). In contrast, GD2xCD3-dHLX BsAb had comparable or lower tumor killing potency as monomeric GD2xCD3 BsAb.

Mouse xenograft studies

A series of mouse xenograft studies were conducted to test the efficacies of GD2xCD3-HDD as compared to GD2xCD3 BsAb *in vivo*. Immunodeficient double knockout (DKO) mice were implanted with subcutaneous neuroblastoma IMR-32 or melanoma M14 cells mixed with peripheral blood mononuclear cells (PBMC) effector cells (see Methods). At day 5 post-implantation, 5 mice per group were given either no treatment, intravenous injections of GD2xCD3 BsAb (6 times per week for 2 weeks), or intravenous injections of GD2xCD3-HDD BsAb (6 times per week for 2 weeks). Tumor volumes and survival data were collected (Fig. 5). The area under the curve (AUC) was calculated for each mouse, and the averages shown in Table 5.

In the case of mice implanted with neuroblastoma IMR-32 cells, administering GD2xCD3 BsAb modestly reduced tumor growth (19% lower AUC, $P = 0.541$), whereas GD2xCD3-HDD treatment on the other hand, significantly diminished tumor growth (65% lower AUC, $P = 0.018$). Survival data at the end of the experiment (155 d post implantation) revealed that in comparison to the 3/5 mice that remained alive in the

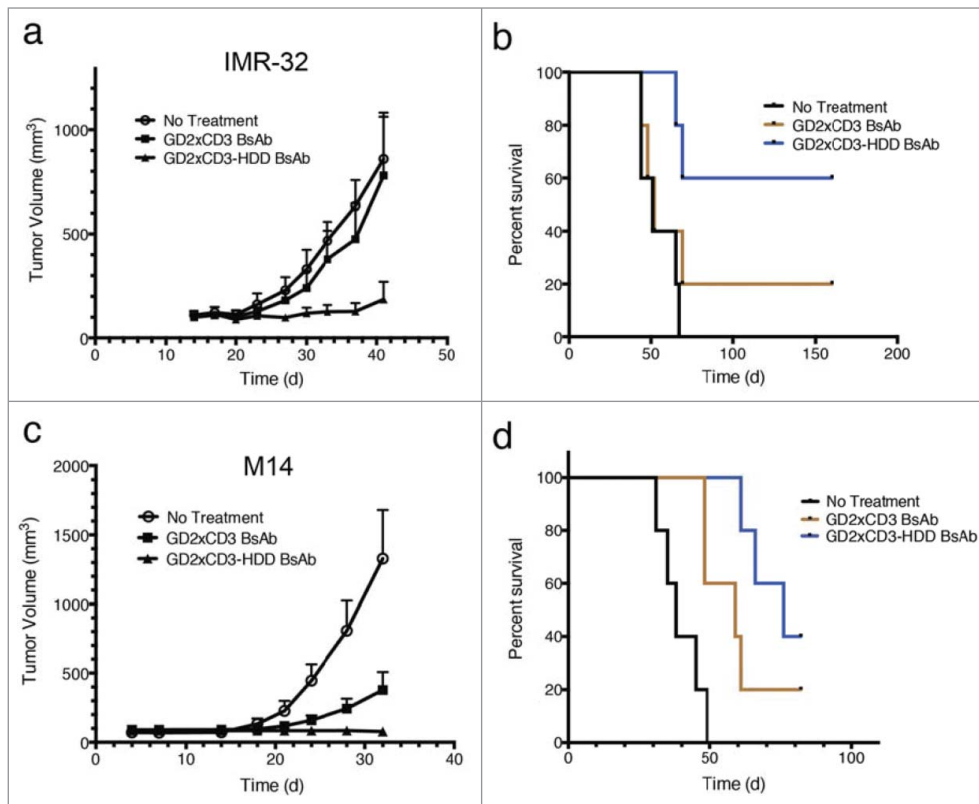


Figure 5. Bispecific antibody treatment affect on tumor growth *in vivo*. Animal xenograft study of neuroblastoma IMR-32 and melanoma M14 tumors mixed with human donor derived peripheral blood mononuclear cells (PBMCs) subcutaneously implanted into immunocompromised double knockout (DKO; BALB-Rag2^{-/-}IL-2R- γ -KO) mice. Recipient mice were treated with BsAbs for 2 weeks and then monitored for tumor growth and survival. (A) Tumor size for mice implanted with IMR-32 cells. (B) Survival of mice implanted with IMR-32 cells. (C) Tumor size for mice implanted with M14 cells. (D) Survival of mice implanted with M14 cells. Data points are shown as the mean \pm SE. Mice were sacrificed for humane reasons if tumor volume exceeded 2 cm³.

GD2xCD3-HDD treatment group, only 1/5 mice survived in the GD2xCD3 group and there were no survivors in the untreated group. In the case of mice implanted with melanoma M14 cells, injection of GD2xCD3 BsAb group markedly reduced tumor growth (57% lower AUC), albeit just beyond statistical significance ($P = 0.065$). The GD2xCD3-HDD treatment again significantly reduced tumor growth (75% lower

Table 5. Analysis of tumor volumes from xenograft-bearing mice treated with the indicated bispecific antibody (BsAb) (mean \pm SD).

IMR-32 xenograft	No treatment	GD2xCD3 BsAb	GD2xCD3-HDD BsAb
AUC(mm ³ xdays)	9127 \pm 4335	7379 \pm 4337	3167 \pm 1270
% change		-19%	-65%
P-value		0.541	0.018
M14 xenograft	No treatment	GD2xCD3 BsAb	GD2xCD3-HDD BsAb
AUC(mm ³ xdays)	9445 \pm 5457	4070 \pm 1389	2339 \pm 1759
% change		-57%	-75%
P-value		0.065	0.024

AUC, $P = 0.024$). Survival data at the end of the experiment (82 d post implantation) found that 2/5 mice remained alive in the GD2xCD3-HDD treated group vs. 1/5 in the GD2xCD3 group and no survivors in the untreated group.

A non-targeting animal mouse xenograft study was also performed using the GD2-negative tumor BV-173 (Fig. S3 and Table S3). The results showed that tumor growth in the mice treated with GD2xCD3-HDD and GD2xCD3 BsAbs were comparable to the non-treated control. Another control mouse experiment was also carried out to examine T-cell retention at the tumor site. Mice were implanted with SH-SY5Y cells expressing a low level of GD2 and were subsequently treated with GD2xCD3-HDD or GD2xCD3 BsAb. This line was chosen to test if the HDD tag may enhance the retention of T cells (resulting in possible excess cytokine release) at the tumor site, without being confounded by enhanced avidity of the BsAb for GD2. Tumors were removed and stained for CD3 (Fig. S4 and Table S4). The data demonstrated no significant difference in T-cell retention at the

tumor site, providing further evidence that the HDD-dimeric BsAb did not differ from the monomeric BsAb in inducing T-cell proliferation or T-cell survival in the absence of a tumor expressing abundant GD2.

Pharmacokinetic analysis

Serum pharmacokinetic analysis was carried out in DKO mice after intravenous injections of BsAbs, in which serum BsAb levels were measured by using an anti-OKT3 and anti-5F11 double sandwich ELISA assay (see Methods). Results are shown in Fig. 6 and Table 6. The C_{max} for GD2xCD3 and GD2xCD3-HDD BsAbs were comparable, at 22.95 and 23.72 μ g/mL, respectively. However, GD2xCD3-HDD BsAb displayed a significantly longer serum half-life ($t_{1/2}$) of 54.68 \pm 17.62 min than GD2xCD3 BsAb (14.04 \pm 10.42 min, $P = 0.002$). There was also a 2-fold increase in sustaining GD2xCD3-HDD BsAb concentrations overtime, as shown by the \sim 2X increased AUC (h \times μ g/mL) relative to the GD2xCD3 BsAb ($P = 0.018$).

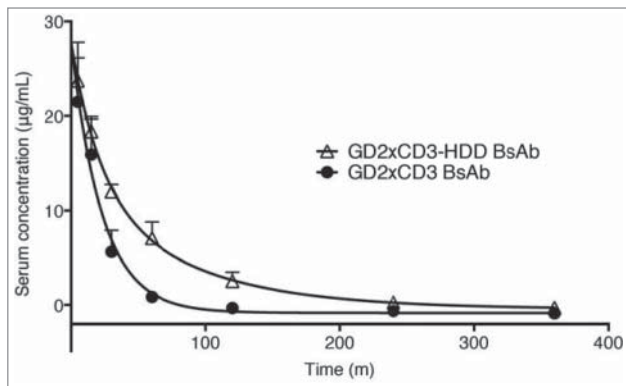


Figure 6. Pharmacokinetics of the indicated bispecific antibody (BsAb) Serum pharmacokinetics of the indicated bispecific antibody (BsAb) in immunocompromised double knockout (DKO; BALB-Rag2^{-/-}IL-2R γ -KO) mice injected with either GD2xCD3 or GD2xCD3-HDD BsAb. Mice were given 50 μ g bolus injection of BsAb, and then tail vein blood was sampled over the course of 6 h for protein clearance, using an anti-5F11 idiotype antibody for detection and sandwich ELISA. Parameters from non-compartmental pharmacokinetic analysis are shown in **Table 6**.

Discussion

Tumors evade T cells by downregulating tumor HLA and by upregulating regulatory T cells, as well as interfering with the homing of cytolytic T cells (CTL), lymphocytes typically comprising low clonal frequency. By engaging CD3 on the surface of T cells, BsAbs activate and redirect polyclonal T cells to tumors, potentially overcoming both issues of insufficient HLA and low clonal frequency in T-cell mediated immunity. In this report, we demonstrated that a tsc-BsAb engineered with the HNF1 α dimerization domain fused to the C-terminus of anti-GD2 x anti-CD3 can induce stable dimers and enhance the functional avidity of the distal scFvs, which are linked to the anti-CD3 scFv by a flexible (GGGG) linker, thereby facilitating bivalent anti-tumor epitope binding. This enhanced avidity resulted in a significant increase in T-cell killing potency (32–37 fold) in cancer cell cytotoxicity assays *in vitro*, and offer significant improvement in tumor ablation efficiency *in vivo*. We hypothesized that anti-CD3 scFvs placed proximal to the HDD tag in the dimeric GD2xCD3-HDD BsAb construct would not behave in a bivalent manner because of steric restrictions from the anti-parallel orientation of helices that compose the HDD. Such an orientation forces the anti-CD3 scFvs in completely opposite directions. The anti-CD3 scFv units were connected to the HDD tag using an antibody hinge region, which further constrained this orientation. We found no evidence of bivalent binding of the HDD-

tagged dimeric tsc-BsAb to CD3 and no enhancement in cytokine release or T-cell proliferation over and above the monomeric tsc-BsAb. We therefore expect that therapeutic use of the HDD tag would not effectively increase cytokine release in patients. Nevertheless, the dimeric GD2xCD3-HDD BsAb displayed enhanced GD2 avidity and killing efficiency *in vitro*, coupled with the increased serum half-life of dimeric BsAbs led to significant tumor reduction in mouse xenograft models of neuroblastoma and melanoma.

We compared the HDD tag to 2 other dimerization domains: dHLX, a synthetic helix-loop-helix domain similar in structure to the HDD tag but incapable of forming homogeneous dimers, and the human Fc domain that also failed to form homogeneous dimers. Neither construct was superior to the HDD tag in T cell-mediated tumor cell killing. This supports the notion that the ideal dimerization domain must be strong enough to pull 2 sets of ScFv fragments together in a stable way, without limiting the flexibility of the anti-CD3 domain to retarget T cells for cancer cell killing. In fact, we have tested a smaller dimerization domain derived from the peptide hormone Endothelin-1, and found that it was not strong enough to form stable dimers when fused to the GD2xCD3 BsAb (data not shown). The HDD tag had the added benefit of functionally monovalent CD3 binding as compared to GD2xCD3-Fc BsAb, the latter showing enhanced binding to CD3. One of the major differences between the GD2xCD3-HDD and GD2xCD3-Fc BsAb is the orientation of the anti-CD3 scFvs accounting for the distinct CD3 avidities.

Since antibodies that bind to carbohydrate antigens such as GD2 are generally of low affinity, the use of stable non-immunogenic peptide sequences to induce homodimerization presents a novel approach to enhance T-cell targeting for cancer immunotherapy. Additionally, dimerization of tsc-BsAbs, which are ~55 kDa in their monomeric form, substantially increase the serum half-life and potential therapeutic efficacy regardless of tumor affinity. The short observed half-life of the monomeric GD2xCD3 BsAb is comparable to that which has been previously reported for tsc-BsAb in mice³¹ and Fab fragments that are similar in size.³² The serum half-life is expected to be substantially longer in humans, based on interspecies scaling.³³ The nearly 4-fold enhancement in serum half-life resulting from the HDD tag is also consistent with enhancement in serum pharmacokinetics observed between F(ab) and F(ab')₂, which are approximately the same sizes as a monomeric and dimeric tsc-BsAb. This limited increase in serum half-life may be more beneficial than the prolonged half-life of a bispecific antibody with an intact Fc domain, which can last in the blood for several weeks due to FcR-mediated recycling^{34,35} and potentiate prolonged

Table 6. Analysis of pharmacokinetics of the indicated bispecific antibody (BsAb) based on non-compartmental analysis (mean \pm SD).

	Half life (min)	Cmax (μ g/mL)	AUC (hr. μ g/mL)	Volume of distribution(mL)	Clearance (mL/hr)
GD2xCD3 BsAb	14.04 \pm 10.42	22.95 \pm 13.07	10.64 \pm 6.42	1.92 \pm 1.01	7.43 \pm 5.90
GD2xCD3-HDD BsAb	54.68 \pm 17.62	23.72 \pm 5.38	22.09 \pm 5.76	2.62 \pm 0.59	2.08 \pm 0.51
fold difference	3.9	1.0	2.1	1.4	0.3
P-value	0.002	0.907	0.018	0.219	0.078

cytokine release. Other methods exist to prolong serum half-life to a narrow range primarily by pegylation (addition of polyethylene glycol polymers), but controversy exists as to whether pegylation itself is immunogenic.³⁶ Addition of the HDD tag presents an effective way to enhance the pharmacokinetic properties of the BsAb with a human-derived tag, which is less likely to be immunogenic. In addition, an HDD tagged dimeric tsc-BsAb may be less likely to cross the blood brain barrier, although addressing this possibility requires further investigation.

In this study, we sought to improve the potency of the tsc-BsAb format to stimulate tumor cell killing, while overcoming some technical limitations by using a simple dimerization strategy. We thus utilized the HDD tag with a BsAb that specifically targets the tumor antigen GD2, an immunogen highly expressed in several metastatic cancer types. Anti-GD2 antibodies have shown long-term safety and efficacy in randomized trials, but one of the major side effects is complement-mediated acute pain occurring during antibody infusion.³⁷ Because GD2xCD3 BsAb lack the Fc portion necessary for complement activation, this strategy of using monomeric or dimeric BsAbs may not be restricted to enhanced tumor cell killing *in vitro* and *in vivo*, but may also be associated with reduced pain as a therapeutic side effect. This dimerization strategy can also be applied to other tsc-BsAbs under clinical development, since it can be easily adopted to enhance tumor binding and to increase serum half-life, with the potential to achieve greater therapeutic efficacy without excess cytokine release.

Methods

Molecular cloning

The sequences of anti-GD2 antibody 5F11²⁰ and humanized anti-CD3³⁸ have previously been reported. 5F11 scFv (VH-VL orientation) and anti-CD3 hOKT3 scFv (VH-VL) with an orientation VHVL were genetically assembled by a 15 amino acid linker ((GGGS)5) and synthesized separately (GenScript, Piscataway, NJ). 5F11scFvs were digested with NheI and ApaI, hOKT3 scFv was digested with ApaI and BamHI, and sequentially ligated into Glutathione synthesis vector (GS) (Invitrogen) to make GD2xCD3 BsAb. Subsequently, 2 cysteine mutations, residue S44C on the heavy chain and residue A100C on the light chain, were introduced by site-directed mutagenesis (Stratagene, CA) to stabilize the 5F11 scFv. Additionally, one affinity maturation mutation P104Y¹⁹ was also incorporated into the 5F11 scFv. The final sequence of the GD2xCD3 BsAb was as follows:

QVQLQQSGPELVKPGASVKISCKTSGYKFTETMHW
VKQSHGKCLEWIGGINPNNGGTNYNQKFKGKATLTV
DKSSSTAYMELRSLTSEDSAVYYCARDTTVPYAYWGQG
TTVTVSSGGGGSGGGSGGGSDIELTQSPAIMSASPG
EKVTMTCSASSISYMHWYQKPGTSPKRWIYDTSKLAS
SVPARFSGSGTSYSLTISMEAEADAATYYCHQRSSYPLT
FGCGTKLEIKRASTKGPGGGGSGGGSGGGGSQVQLV
QSGGGVVQPGRSLRLSCKASGYTFTRYTMHWVRQAPG
KGLEWIGYINPSRGYTNYNQKFKDRFTISRDNKNTAFL
QMDSLRLPEDTGVYFCARYYDDHYCLDYWGQGTPTVTS

SGGGGSGGGGSGGGGSDIQMTQSPSSLSASVGDRTTIT
CSASSVSVMNWIYQTPGKAPKRWIYDTSKLASGVPSTRF
SGSGSGTDYFTFTISLQPEDIAITYCQQWSSNPFTFGQG
TKLQITR.

To construct the GD2xCD3-HDD BsAb, the following sequences were added to the C-terminus of the GD2xCD3 BsAb: IgG3 hinge (TPLGDTTHTSG), HNF1 α dimerization domain (MVKLSQLQTELLAALLESGLSKEALIQALGE), and a spacer (GSGGAP).

For the GD2xCD3-Fc BsAb construct, a human IgG1 hinge domain and Fc sequence were added to the sequence of GD2xCD3 BsAb.

The sequence of the GD2xCD3-dHLX was identical to GD2xCD3-HDD, except the HNF1 α dimerization domain was replaced with the helix-loop-helix motif (GELEELLKHLKELLKG-PRK-GELEELLKHLKELLK).^{23,39}

For the GD2xCD3-Fc BsAb construct, a human IgG1 hinge domain and Fc sequence was added to the C-terminus of the GD2xCD3 BsAb sequence.

Production and purification

Expression constructs were made with the DNA of GD2xCD3, GD2xCD3-HDD, or GD2xCD3-dHLX BsAb followed by a 6 \times His tag. An expression construct with GD2xCD3-Fc was also made, with no additional purification tags. DNA was transfected into DG44 CHO-S cells (Invitrogen) by electroporation using a Nucleofector II electroporation machine (Amaxa) and nucleofection solution V. Transfected cells were subject to drug selection with 500 μ g/mL G418. Two weeks later, single cells were plated in 96-wells by serial dilution. Irradiated CHO-S cells (5000/per well) were used as feeder cells. Supernatants from each clone were harvested in 3 weeks, and subject to GD2 binding assay. Clones with the highest binding to GD2 were picked, scaled up for large culture via orbital shaking at 125 rpm in 37°C (8% CO₂) and cultured until the cells reach 2 million cells/mL and are in log-phase growth. Cultures were harvested when the desired antibody yield was achieved or when the viability dropped to <40%. BsAb proteins with 6 \times His tags secreted into the culture supernatant were subsequently affinity purified by Ni²⁺ sepharose (GE Healthcare Bio-Sciences, Sweden), eluted with 300 mM imidazole, dialyzed in PBS pH 7.4, and purified by size exclusion chromatography (Superdex 200 GL column, GE Healthcare Bio-Sciences). BsAbs with an Fc domain were purified by affinity chromatography using MabSelect resin (GE Healthcare Bio-Sciences). The hydrodynamic radii of the sample solution were measured by dynamic light scattering using a Malvern Zetasizer Nano (Malvern Instruments, Worcestershire, UK). Sample purity was also evaluated by size-exclusion high-performance liquid chromatography (SE-HPLC). Approximately 20 μ g of protein was injected into a TSK-GEL G3000SWXL 7.8 mm \times 30 cm, 5 μ m column (TOSOH Bioscience) with 0.4 M NaClO₄, 0.05 M NaH₂PO₄, pH 6.0 buffer at flow rate of 0.5 mL/min, and UV detection at 280 nm. Ten microliters of gel-filtration standard (Bio-Rad) was analyzed in parallel for MW markers.

ELISA

To assay GD2 binding, GD2 antigen was first coated at 1 $\mu\text{g}/\text{mL}$ per well in 90% ethanol on vinyl 96-well plates at room temperature (RT) overnight. On the subsequent day, after blocking the plates with 150 $\mu\text{L}/\text{well}$ 0.5% bovine serum albumin (BSA), a dilution series of the BsAb antibodies were added to the plates and incubated at RT for 2 h. Plates were washed with PBS and 100 $\mu\text{L}/\text{well}$ of mouse-anti-His-tag antibody (AbD Serotec; dilute 1:1000 dilution in 0.5% BSA) were added and incubated for another hour. Lastly, 100 $\mu\text{L}/\text{well}$ goat-anti-mouse-HRP antibody (Jackson ImmunoResearch; 1:3000 dilutions in 0.5% BSA) were added and incubated for 1 h. Plates were developed using 150 $\mu\text{L}/\text{well}$ OPD buffer (Sigma) and read at 490 nm on a spectrophotometer.

T-cell binding by fluorescence cytometry

T cells were expanded using CD3/CD28 beads. BsAbs were incubated with 1×10^6 T cells per sample for 30 min on ice. After washing, the T cells were reacted with a anti-huOKT3-scFv-mouseFc antibody (Laboratory of Dr. Nai-Kong Cheung, Memorial Sloan Kettering, New York, NY) at 1 μg per 1×10^6 cells on ice for 30 min, washed, and then reacted with a goat anti-mouse R-Phycoerythrin (PE)-conjugated antibody (Jackson Immuno Research) for 20 min. T cells were washed and analyzed by fluorescence cytometry on a FACS Calibur (BD Biosciences, San Jose, CA).

In vitro binding kinetics by Biacore T-100 Biosensor (GE Healthcare)

A Biacore T-100 Biosensor, a CM5 sensor chip, and related reagents were all purchased from GE Healthcare. The ganglioside GM1 was obtained from ALEXIS Biochemicals (AXXORA L.L. C.) and GD2 was from Advanced ImmunoChemical. Gangliosides were directly immobilized onto the CM5 sensor chip via hydrophobic interaction, as previously described.¹⁹ The active surface contained a 1:1 mixture of GD2 and GM1, and the reference surface contained only GM1. BsAb samples were diluted in HBS-EP buffer (0.01 M HEPES pH 7.4, 0.15 M NaCl, 3 mM EDTA, 0.05% v/v Surfactant P20) at varying concentrations and injected onto the sensor surface at a flow rate of 30 $\mu\text{L}/\text{min}$ over 1–2 min. Following completion of the association phase, dissociation was monitored in HBS-EP buffer for 3 min at the same flow rate. At the end of each cycle, the surface was regenerated using 10–20 mM NaOH at a flow rate of 50 $\mu\text{L}/\text{min}$ over 1 min. The data were analyzed using the Biacore T-100 evaluation software, and the apparent association on rate constant (kon), dissociation off rate constant (koff) and equilibrium dissociation constant ($K_D = \text{koff}/\text{kon}$) were calculated.

Cell lines

The neuroblastoma cell line LAN1 and the melanoma line M14 were obtained from University of California, Los Angeles. Neuroblastoma IMR-32 cells (from which SKNLD is derived) and the SH-SY5Y cell line were obtained from American Tissue Type Culture Collection (ATCC). Leukemia cell line BV-173

was obtained from the laboratory of Dr. Richard J. O'Reilly (Memorial Sloan Kettering, New York NY). Authentication of cell lines was accomplished by short tandem repeat (STR) DNA sequencing. Cells were cultured in RPMI1640 (Cellgro) supplemented with 10% FBS (Life Technologies) at 37°C in a 5% CO₂ humidified incubator.

Cytokine release assay

Peripheral blood mononuclear cells (PBMC) were isolated from healthy donor blood by lymphocyte separation medium (Mediatech) centrifugation. Human T cells were purified by Pan T Cell Isolation Kit (Miltenyi Biotec). T cells (50000/per well) was co-cultured with neuroblastoma cell IMR-32 cell (10,000/per well) in the presence of BsAb in 37°C in a 96-well plate. Supernatants were harvested at 24 h and the concentrations of 4 different cytokines (IL-2, IL-10, IFN γ and TNF α) were assessed using an ELISA-based cytokine assay kit (OptEIA™ human cytokine set, BD Biosciences). The assay was run according to the manufacturer's protocol and cytokine levels were quantitated using the standards supplied from the kit. Positive control samples were run using T cells activated with CD3/CD28 immunobeads to verify that cytokines could be adequately detected.

T cell proliferation assay

T cells were purified from human PBMC using the Pan T Cell Isolation Kit (Miltenyi Biotec). Neuroblastoma cells IMR-32 were irradiated at 80 Gy and resuspended in RPMI (GIBCO) at 0.1 million/mL. The IMR-32 cells were mixed at 1×10^4 cells/well (100 μL) with 2×10^5 purified T cells (100 μL) in the presence of different antibodies (50 μL) added to 96-well cell culture plate to a final volume of 250 $\mu\text{L}/\text{well}$. T cells were cultured and maintained in RPMI supplemented with FBS in 37°C for 6 d and T-cell proliferation was quantitated using Cell Counting Kit-8 (CCK-8) (Dojindo Mol) assay according to manufacturer's protocol.

Cell cytotoxicity (chromium⁵¹ release assay)

T cells were purified from human PBMC using the Pan T Cell Isolation Kit (Miltenyi Biotec). CD3/CD28 dynabeads (Invitrogen) were then used to stimulate and expand T cells according to manufacturer's protocol. Expanded T cells were cultured and maintained in RPMI supplemented with FBS and 30 U/mL IL-2. The resultant population of T cells was stained with anti-CD3-perCP Cy5.5, anti-CD4-fluorescein isothiocyanate (FITC), anti-CD8-allophycocyanin (APC), and anti-CD56-PE antibodies (BD Biosciences) and analyzed using a FACS Calibur.

Target tumor cells were harvested with trypsin/EDTA and labeled with sodium⁵¹Cr chromate (Amersham, Arlington Height, IL) at 100 $\mu\text{Ci}/10^6$ cells at 37°C for 1 h. After the cells were washed twice, 5000 target cells/well were admixed with 50,000 effector cells and BsAb antibodies in 96-well polystyrene round-bottom plates (BD Biosciences) to a final volume of 250 $\mu\text{L}/\text{well}$. Samples were prepared in triplicate. The plates were incubated at 37°C for 4 h and then centrifuged at 800 g for 10 min after which ⁵¹Cr release into the supernatant was counted

using a γ -counter (Packed Instrument, Downers Grove, IL). The percentage of specific release was calculated using the formula: 100% (experimental cpm- background cpm) / (10% sodium dodecyl sulfate [SDS] cpm-background CPM), in which cpm are counts per minute of ^{51}Cr released, total release was assessed by lysis with 10% sodium dodecyl sulfate (SDS; Sigma, St Louis, Mo), and background release was measured in the absence of effector cells.

Xenograft mouse model

The immune deficient mouse strain BALB-Rag2^{-/-}IL-2R γ c-KO (DKO) was kindly provided by Dr. Mamoru Ito, Central Institute for Experimental Animals, Kawasaki, Japan and maintained at Memorial Sloan Kettering Cancer Center. Animals were provided with Sulfatrim chow. All procedures were performed in accordance with the protocols approved by our Institutional Animal Care and Use Committee and institutional guidelines for the proper and human use of animals in research. *In vivo* experiments were performed in 6–10 week old mice bred at the Memorial Sloan Kettering Cancer Center. PBMC of healthy donors were isolated from whole human blood from healthy donor (New York blood Center). Erythrocytes were depleted by incubation for 15 min with erythrocyte lysis buffer (Lonza) and thrombocytes removed by supernatant aspiration following centrifugation at 100 \times g for 10 minutes. All PBMC samples used had similar percentages of T-cell subpopulations (30–50% CD3 positive). Purified PBMC were mixed with tumor cells (1:1 ratio) and implanted in DKO mice subcutaneously. Treatment with BsAb was initiated at day 5. Mice were treated with 10 $\mu\text{g/day}$ of antibody for 2 consecutive weeks (6 d per week). Tumor size was measured by caliper twice per week; both tumor length and width was recorded. Mice were sacrificed if tumor volumes reached 2 cm^3 .

Tumor immunohistochemistry

Tumor sectioning and immunohistochemistry were done at the Molecular Cytology Core Facility of Memorial Sloan Kettering Cancer Center. Paraffin embedded tumor sections were stained for CD3 using Discovery XT processor (Ventana Medical Systems). A rabbit polyclonal anti-CD3 antibody (Dako) was used at a concentration of 1.2 $\mu\text{g/mL}$. Preceding the primary antibody incubation, the tissue sections were blocked for 30 min

in 10% normal goat serum, 2% BSA in PBS. The incubation with the primary antibody was done for 3 h, followed by 1 h incubation with biotinylated goat anti-rabbit IgG (Vector labs,) at 1:200 dilution. Secondary Antibody Blocker, Blocker D, streptavidin-HRP and DAB detection kit (Ventana Medical Systems) were used according to the manufacturer instructions. Cell staining quantitation was done using MetaMorph (Molecular Devices).

Pharmacokinetics

Blood was obtained from tail vein of DKO mice over 6 h after a bolus injection of 50 μg of BsAb. Serum BsAb levels were measured by double sandwich ELISA where BsAb was captured using solid phase human anti-OKT3 antibody (20 $\mu\text{g/mL}$), and bound BsAb was detected using 5 $\mu\text{g/mL}$ rat anti-5F11 idiotype antibody, followed by mouse anti-rat IgG-HRP antibody at 1:1000 (Jackson ImmunoResearch, West Grove, PA). Pharmacokinetic analysis was carried out by non-compartmental analysis of the serum concentration-time data using WinNonlin software program (Pharsight Corp., Mountain View, CA).

Statistics

Binding data and dose response curves were fitted by non-linear regression using GraphPad Prism software, to allow determination of EC50. For comparison of curves, best-fit values for EC50 were analyzed for significance using F tests. Significance of tabulated data were determined by Student's t-test, and $P < 0.05$ was considered statistically significant. For comparison of different BsAb constructs, molar equivalents were considered be each unit that contained one anti-GD2 domain and one anti-CD3 domain.

Disclosure of Potential Conflicts of Interest

MA and NKC were named as inventors in a patent application for multimerization technologies filed by Memorial Sloan Kettering Cancer Center.

Acknowledgments

We thank Dr. Jian Hu for running the affinity measurements on Biacore, and Dr. Hong Xu, Hong-fen Guo, Hoa Tran and Yi Feng for excellent technical assistance.

References

- Choi BD, Cai M, Bigner DD, Mehta AI, Kuan CT, Sampson JH. Bispecific antibodies engage T cells for antitumor immunotherapy. *Expert Opin Biol Ther* 2011; 11:843-53; PMID:21449821; <http://dx.doi.org/10.1517/14712598.2011.572874>
- Dreier T, Baeuerle PA, Fichtner I, Grün M, Schlereth B, Lorenczewski G, Kufer P, Lutterbüse R, Riethmüller G, Gjørstrup P, et al. T cell costimulus-independent and very efficacious inhibition of tumor growth in mice bearing subcutaneous or leukemic human B cell lymphoma xenografts by a CD19-/CD3- bispecific single-chain antibody construct. *J Immunol* 2003; 170:4397-402; PMID:12682277; <http://dx.doi.org/10.4049/jimmunol.170.8.4397>
- Bargou R, Leo E, Zugmaier G, Klinger M, Goebeler M, Knop S, Noppeney R, Viardot A, Hess G, Schuler M, et al. Tumor regression in cancer patients by very low doses of a T cell-engaging antibody. *Science* 2008; 321:974-7; PMID:18703743; <http://dx.doi.org/10.1126/science.1158545>
- Topp MS, Kufer P, Gökbuğut N, Goebeler M, Klinger M, Neumann S, Horst HA, Raff T, Viardot A, Schmid M, et al. Targeted therapy with the T-cell-engaging antibody blinatumomab of chemotherapy-refractory minimal residual disease in B-lineage acute lymphoblastic leukemia patients results in high response rate and prolonged leukemia-free survival. *J Clin Oncol* 2011; 29:2493-8; PMID:21576633; <http://dx.doi.org/10.1200/JCO.2010.32.7270>
- Torisu-Itakura H, Schoellhammer HF, Sim MS, Irie RF, Hausmann S, Raum T, Baeuerle PA, Morton DL. Redirected lysis of human melanoma cells by a MCSP/CD3-bispecific BiTE antibody that engages patient-derived T cells. *J Immunother* 2011; 34:597-605; PMID:21904216; <http://dx.doi.org/10.1097/CJI.0b013e3182307f8d>
- Cioffi M, Dorado J, Baeuerle PA, Heeschen C. EpCAM/CD3-Bispecific T-cell engaging antibody MT110 eliminates primary human pancreatic cancer stem cells. *Clin Cancer Res* 2012; 18:465-74; PMID:22096026; <http://dx.doi.org/10.1158/1078-0432.CCR-11-1270>
- Osada T, Hsu D, Hammond S, Hobeika A, Devi G, Clay TM, Lysterly HK, Morse MA. Metastatic colorectal cancer cells from patients previously treated with chemotherapy are sensitive to T-cell killing mediated by CEA/CD3-bispecific T-cell-engaging BiTE antibody. *Br J Cancer* 2010; 102:124-33; PMID:19953093; <http://dx.doi.org/10.1038/sj.bjc.6605364>
- Lutterbüse R, Raum T, Kischel R, Hoffmann P, Mangold S, Rattel B, Friedrich M, Thomas O, Lorenczewski G, Rau D, et al. T cell-engaging BiTE antibodies

- specific for EGFR potently eliminate KRAS- and BRAF-mutated colorectal cancer cells. *Proc Natl Acad Sci U S A* 2010; 107:12605-10; PMID:20616015; <http://dx.doi.org/10.1073/pnas.1000976107>
9. Cuesta AM, Sainz-Pastor N, Bonet J, Oliva B, Alvarez-Vallina L. Multivalent antibodies: when design surpasses evolution. *Trends Biotechnol* 2010; 28:355-62; PMID:20447706; <http://dx.doi.org/10.1016/j.tibtech.2010.03.007>
 10. Narayana N, Hua Q, Weiss MA. The dimerization domain of HNF-1alpha: structure and plasticity of an intertwined four-helix bundle with application to diabetes mellitus. *J Mol Biol* 2001; 310:635-58; PMID:11439029; <http://dx.doi.org/10.1006/jmbi.2001.4780>
 11. Cheung NK, Saarinen UM, Neely JE, Landmeier B, Donovan D, Coccia PF. Monoclonal antibodies to a glycolipid antigen on human neuroblastoma cells. *Cancer Res* 1985; 45:2642-9; PMID:2580625
 12. Chang HR, Cordon-Cardo C, Houghton AN, Cheung NK, Brennan MF. Expression of disialogangliosides GD2 and GD3 on human soft tissue sarcomas. *Cancer* 1992; 70:633-8; PMID:1623478; [http://dx.doi.org/10.1002/1097-0142\(19920801\)70:3%3c633::AID-CNCR2820700315%3e3.0.CO;2-F](http://dx.doi.org/10.1002/1097-0142(19920801)70:3%3c633::AID-CNCR2820700315%3e3.0.CO;2-F)
 13. Grant SC, Kostakoglu L, Kris MG, Yeh SD, Larson SM, Finn RD, Oettgen HF, Cheung NV. Targeting of small-cell lung cancer using the anti-GD2 ganglioside monoclonal antibody 3F8: a pilot trial. *Eur J Nuclear Med* 1996; 23:145-9; PMID:8925848; <http://dx.doi.org/10.1007/BF01731837>
 14. Liang YJ, Ding Y, Lavery SB, Lobaton M, Handa K, Hakomori SI. Differential expression profiles of glycosphingolipids in human breast cancer stem cells vs. cancer non-stem cells. *Proc Natl Acad Sci U S A* 2013; 110:4968-73; PMID:23479608; <http://dx.doi.org/10.1073/pnas.1302825110>
 15. Battula VL, Shi Y, Evans KW, Wang RY, Spaeth EL, Jacamo RO, Guerra R, Sahin AA, Marini FC, Hortobagyi G, et al. Ganglioside GD2 identifies breast cancer stem cells and promotes tumorigenesis. *J Clin Invest* 2012; 122:2066-78; PMID:22585577; <http://dx.doi.org/10.1172/JCI59735>
 16. Yanagisawa M, Yoshimura S, Yu RK. Expression of GD2 and GD3 gangliosides in human embryonic neural stem cells. *ASN Neuro* 2011; 3:pii: e00054; PMID:21395555; <http://dx.doi.org/10.1042/AN20110006>
 17. Martinez C, Hofmann TJ, Marino R, Dominici M, Horwitz EM. Human bone marrow mesenchymal stromal cells express the neural ganglioside GD2: a novel surface marker for the identification of MSCs. *Blood* 2007; 109:4245-8; PMID:17264296; <http://dx.doi.org/10.1182/blood-2006-08-039347>
 18. Jin HJ, Nam HY, Bae YK, Kim SY, Im IR, Oh W, Yang YS, Choi SJ, Kim SW. GD2 expression is closely associated with neuronal differentiation of human umbilical cord blood-derived mesenchymal stem cells. *Cell Mol Life Sci* 2010; 67:1845-58; PMID:20165901; <http://dx.doi.org/10.1007/s00018-010-0292-z>
 19. Hu J, Huang X, Ling CC, Bundle DR, Cheung NK. Reducing epitope spread during affinity maturation of an anti-ganglioside GD2 antibody. *J Immunol* 2009; 183:5748-55; PMID:19812201; <http://dx.doi.org/10.4049/jimmunol.0901409>
 20. Cheung NK, Modak S, Lin Y, Guo H, Zanzonico P, Chung J, Zuo Y, Sanderson J, Wilbert S, Theodore LJ, et al. Single-chain Fv-streptavidin substantially improved therapeutic index in multistep targeting directed at disialoganglioside GD2. *J Nucl Med* 2004; 45:867-77; PMID:15136638
 21. Cheng M, Ahmed M, Xu H, Cheung NKV. Structural design of disialoganglioside GD2 and CD3-bispecific antibodies to redirect T cells for tumor therapy. *Int J Cancer* 2014; 136(2):476-86; PMID:24895182; <http://dx.doi.org/10.1002/ijc.29007>
 22. Woodle ES, Thistlethwaite JR, Jolliffe LK, Zivin RA, Collins A, Adair JR, Bodmer M, Athwal D, Alegre ML, Bluestone JA. Humanized OKT3 antibodies: successful transfer of immune modulating properties and idiotype expression. *J Immunol* 1992; 148:2756-63; PMID:1533410
 23. Pluckthun A, Pack P. New protein engineering approaches to multivalent and bispecific antibody fragments. *Immunotechnology* 1997; 3:83-105; PMID:9237094; [http://dx.doi.org/10.1016/S1380-2933\(97\)00067-5](http://dx.doi.org/10.1016/S1380-2933(97)00067-5)
 24. Holliger P, Prospero T, Winter G. "Diabodies": small bivalent and bispecific antibody fragments. *Proc Natl Acad Sci U S A* 1993; 90:6444-8; PMID:8341653; <http://dx.doi.org/10.1073/pnas.90.14.6444>
 25. Kipriyanov SM, Moldenhauer G, Schuhmacher J, Cochlovius B, Von der Lieth CW, Matys ER, Little M. Bispecific tandem diabody for tumor therapy with improved antigen binding and pharmacokinetics. *J Mol Biol* 1999; 293:41-56; PMID:10512714; <http://dx.doi.org/10.1006/jmbi.1999.3156>
 26. Staerz UD, Bevan MJ. Hybrid hybridoma producing a bispecific monoclonal antibody that can focus effector T-cell activity. *Proc Natl Acad Sci U S A* 1986; 83:1453-7.
 27. Ridgway JB, Presta LG, Carter P. 'Knobs-into-holes' engineering of antibody CH3 domains for heavy chain heterodimerization. *Protein Eng* 1996; 9:617-21; PMID:8844834; <http://dx.doi.org/10.1093/protein/9.7.617>
 28. Rossi DL, Rossi EA, Cardillo TM, Goldenberg DM, Chang CH. A new class of bispecific antibodies to redirect T cells for cancer immunotherapy. *MAbs* 2014; 6:381-91; PMID:24492297; <http://dx.doi.org/10.4161/mabs.27385>
 29. Molhoj M, Crommer S, Brischwein K, Rau D, Sriskandarajah M, Hoffmann P, Kufer P, Hofmeister R, Baeuerle PA. CD19-/CD3-bispecific antibody of the BiTE class is far superior to tandem diabody with respect to redirected tumor cell lysis. *Mol Immunol* 2007; 44:1935-43; PMID:17083975; <http://dx.doi.org/10.1016/j.molimm.2006.09.032>
 30. Asano R, Ikoma K, Shimomura I, Taki S, Nakanishi T, Umetsu M, Kumagai I. Cytotoxic enhancement of a bispecific diabody by format conversion to tandem single-chain variable fragment (taFv): the case of the hEx3 diabody. *J Biol Chem* 2011; 286:1812-8; PMID:21097496; <http://dx.doi.org/10.1074/jbc.M110.172957>
 31. Schlereth B, Fichtner I, Lorenczewski G, Kleindienst P, Brischwein K, da Silva A, Kufer P, Lutterbuese R, Junghahn I, Kasimir-Bauer S, et al. Eradication of tumors from a human colon cancer cell line and from ovarian cancer metastases in immunodeficient mice by a single-chain Ep-CAM-/CD3-bispecific antibody construct. *Cancer Res* 2005; 65:2882-9; PMID:15805290; <http://dx.doi.org/10.1158/0008-5472.CAN-04-2637>
 32. Covell DG, Barbet J, Holton OD, Black CD, Parker RJ, Weinstein JN. Pharmacokinetics of monoclonal immunoglobulin G1, F(ab')2, and Fab' in mice. *Cancer Res* 1986; 46:3969-78; PMID:3731067
 33. Grene-Lerouge NA, Bazin-Redureau MI, Debray M, Scherrmann JM. Interspecies scaling of clearance and volume of distribution for digoxin-specific Fab. *Toxicol Appl Pharmacol* 1996; 138:84-9; PMID:8658517; <http://dx.doi.org/10.1006/taap.1996.0101>
 34. Giragossian C, Clark T, Piche-Nicholas N, Bowman CJ. Neonatal Fc receptor and its role in the absorption, distribution, metabolism and excretion of immunoglobulin G-based biotherapeutics. *Curr Drug Metab* 2013; 14:764-90; PMID:23952252; <http://dx.doi.org/10.2174/13892002113149990099>
 35. Wang W, Wang EQ, Balthasar JP. Monoclonal antibody pharmacokinetics and pharmacodynamics. *Clin Pharmacol Ther* 2008; 84:548-58; PMID:18784655; <http://dx.doi.org/10.1038/clpt.2008.170>
 36. Schellekens H, Hennink WE, Brinks V. The immunogenicity of polyethylene glycol: facts and fiction. *Pharm Res* 2013; 30:1729-34; PMID:23673554; <http://dx.doi.org/10.1007/s11095-013-1067-7>
 37. Sorkin LS, Otto M, Baldwin WM 3rd, Vail E, Gillies SD, Handgretinger R, Barfield RC, Ming Yu H, Yu AL. Anti-GD(2) with an FC point mutation reduces complement fixation and decreases antibody-induced allodynia. *Pain* 2010; 149:135-42; PMID:20171010; <http://dx.doi.org/10.1016/j.pain.2010.01.024>
 38. Adair JR, Athwal DS, Bodmer MW, Bright SM, Collins AM, Pulito VL, Rao PE, Reedman R, Rothermel AL, Xu D, et al. Humanization of the murine anti-human CD3 monoclonal antibody OKT3. *Hum Antibodies Hybridomas* 1994; 5:41-7; PMID:7858182
 39. Hill RB, DeGrado WF. Solution structure of alpha2D, a natively like de novo designed protein. *J Am Chem Soc* 1998; 120:1138-45; <http://dx.doi.org/10.1021/ja9733649>